Magnesium and Magnesium Alloy Foams

T. R. Neu[1], M. Mukherjee[2], F. Garcia-Moreno[1,2], J. Banhart[1,2]
[1]Technische Universität Berlin, Hardenbergstrasse 36, 10623 Berlin, Germany
[2]Helmholtz Centre Berlin, Hahn Meitner Platz 1, 14109 Berlin, Germany

Abstract

In this article we report the required conditions for production of Mg and Mg-Al alloy foams starting from metallic powders. Al content was varied from 0 to 17 wt.%. Uniaxial hot pressing and extrusion were used to prepare foamable precursors both with and without blowing agent. Foaming was performed under argon atmosphere. Two different foaming techniques were employed: conventional foaming under 1 bar and Pressure Induced Foaming (PIF). Foaming process was monitored in-situ by X-ray radioscopy. Foams were evaluated in terms of their volume expansion and macrostructure.

1 Introduction

Among all available metal foams aluminium foams are the most preferred ones due to their light weight. But the use of magnesium instead of aluminium can make foams even lighter due to its low density: 1.74 gcm^{-3} compared to 2.7 $g.cm^{-3}$ for aluminium. In addition, for a given density Mg foams show greater strength than Al foams [1]. Hence for light-weight construction Mg foams have even greater potential than Al foams.

Mg foams are also being considered as biomaterial because Mg is biocompatible and biodegradable. The porosity level of foam can be adjusted in order to match the strength and Young's modulus of the body parts, and the cellular structure foams can assist in better integration of the implants with natural tissues [2,4]. However, due to its low corrosion resistance Mg implants degrade in less the time required for growth of tissues [2]. Some alloying elements, e.g., Al, are often used to slow down degradation of Mg [2,5]. Therefore foams made from Mg-Al alloys are also of significant importance.

In spite of having such potential research activities on Mg foams production are small. This is mainly because of the high reactivity of Mg. The reported manufacturing routes for closed-cell Mg foams are direct foaming of melt [6], high pressure casting for integral foam [7], vacuum foaming of Mg slurries [8], and casting [9] and space holder method [3] to produce open-cell Mg foams. The powder metallurgical (PM) route, i.e., melting of powder compacts, is one of the most important ones for foam production because it allows for processing of a wide range component geometries. Till date only Bach et al. have investigated Mg-3wt.Zn foams by PM route [10]. In this article we report the production of Mg and Mg-Al alloy foams by PM route.

2 Experimental Procedure / Materials and Method

2.1 Materials

Magnesium (Carl Roth, 99.8% pure, $D_{100} < 75$ µm), aluminium (Alpoco, 99.7% pure, $D_{100} < 100$ µm) and powdered TiH_2 serving as blowing agent (Chemetall, Grade N, 98.8% pure, $D_{100} < 63$ µm) were used to prepare foamable precursors. The TiH_2 was heat-treated at 480 °C for 180 min in air in order to shift the hydrogen release range to higher temperatures, which is essential for a good foam structure [11,12]. Precursors were prepared both with and without TiH_2. The alloys used in this study are given in Table 1. In the case of precursors containing more than one type of powder, the powders were mixed for 25 min in air. Two methods were employed for consolidation: uniaxial pressing and extrusion. For uniaxial pressing 20–25 g of powder blend were subjected to 300 MPa pressure for 15 min at 400 °C. Cylindrical tablets of 36 mm diameter were obtained from which $10\times10\times4$ mm^3 large samples were cut out for foaming. For extrusion, at first 55–70 g of powder blend were uniaxially compacted at room temperature into cylindrical billets of 28 mm diameter applying 100 MPa pressure. These rods then were extruded at 300 °C applying indirect extrusion. The diameter of the extruded rods was 9.5 mm. 8-mm long pieces were cut from these rods for foaming. The density of the precursor was measured by Archimedes' principle, using a Sartorius YDK 01 balance and Ethanol as buoyant.

2.2 Foaming procedure

Magnesium readily oxidises if foamed in ambient atmosphere. To avoid this all the foamings in this study was performed under argon atmosphere. For this a gas-tight X-ray transparent furnace was used which allowed for foaming under controlled gas atmosphere and pressure. This furnace had a ceramic heating plate. Samples were inserted inside a steel section (16×16 mm^2 cross section), which was placed on top of the heating plate. This steel tube prevented reaction between the sample and the ceramic heating plate during foaming. Temperature was measured at the bottom surface of the steel tube by a thermocouple that was led through a hole in the heating plate. A suitable foaming temperature was determined beforehand by using additional calibration experiments as described in Ref. [13]. The foaming temperature for each alloy was about 100 K above the liquidus temperature of that alloy.

Before heating the sample, the furnace first was evacuated to 1 mbar and then was backfilled with argon up to 1.5 bar. This sequence was carried out five times. In the last cycle the furnace was filled with argon only up to 1.2 bar [14]. Foaming was performed by heating the precursor to a pre-determined foaming temperature, after which the temperature was held isothermally 150 s followed by natural cooling. Such conditions are labelled as "ambient pressure". Another foaming method was employed, which is known as "Pressure Induced Foaming" (PIF) [15]. For this, the evacuation-filling sequence was performed the same way as explained earlier except in the last cycle argon was filled up to 10 bar. Precursor was melted under this high pressure. After melting, the gas pressure was released to 1 bar. Cooling was initiated immediately after the pressure level reached 1 bar.

Foaming was continuously monitored in situ by using an X-ray radioscopy set-up comprising a microfocus X-ray source and a panel detector [16]. In this work, the X-ray spot size was set to 5 µm by applying 100 kV voltage, leading to 100 µA current. Foam expansion was determined by analysing X-ray images with the dedicated software AXIM [16]. After solidification, foams were sectioned and polished, and then photographed.

Table 1. Alloys, experimental conditions and foam quality (Uni – Uniaxial, Ext – Extrusion, VEF – volume expansion factor). The resulting foam quality for each experimental condition is represented by four parameters, which are indicated by four characters (+ or -) in each cell of the table. The first and second characters indicate maximum and end expansion, respectively. The third and fourth characters indicate the quality of foam structure in liquid (seen in X-ray images) and solid state, respectively. For the first place, "+" is for VEF≥ 2.5, "-" is for VEF<2.5. For the second place, "+" is for VEF≥ 2, "-" is for VEF<2. For both of the third and fourth places, "+" means a "good" foam structure, whereas"-" suggests the opposite.

TiH_2 (yes/no) →	With TiH_2 (0.5 wt.%)				Without TiH_2			
Foaming condition →	Ambient pressure		PIF (10 bar)		Ambient pressure		PIF (10 bar)	
Compaction →	Uni	Ext	Uni	Ext	Uni	Ext	Uni	Ext
Alloy (melting range) ↓								
Mg (650 °C)	----	+-+-	----	++++	----	----	----	--+-
MgAl3 (635–600 °C)	----	+-+-	----	++++	No experiment			
MgAl10 (600–480 °C)	----	+-+-	----	++++	----	----	+---	++++
MgAl17 (555–437 °C)	----	+-+-	+++-	++++	----	----	++--	++++

3 Results

3.1 Density and expansion

Relative densities of precursors were determined by relating the measured densities to the theoretical densities of the alloy involved and are given in Figure 1. All the values in Figures 1–3 are averages of three measurements and the error bars represents standard deviation. For pure Mg, the density of extruded samples was higher than that of uniaxially compressed samples. The density of the latter increased with Al content, whereas the density of extruded samples either remained the same or slightly decreased.

Figures 2 and 3 show the maximum (in the liquid state) and final (in the solid state) expansion of all foams. The expansion and qualities of foam structure for all the alloys are summarized in Table 1. The nomenclature used in Figures 2–6 is as follows. "PIF" – pressure induced foaming method PIF, "TiH_2" – precursor contains TiH_2, No PIF – foaming under ambient pressure, and No TiH_2 – precursor does not contain TiH_2. In general, extruded samples expanded more than uniaxially pressed samples. For both, foam expansion increased with Al content. For the uniaxially pressed samples, there was almost no expansion for Mg and MgAl3, but two other alloys showed some expansion but only when PIF method was used. The extruded samples apart from "No PIF, No TiH_2" expanded and reached porosities of 60–70%.

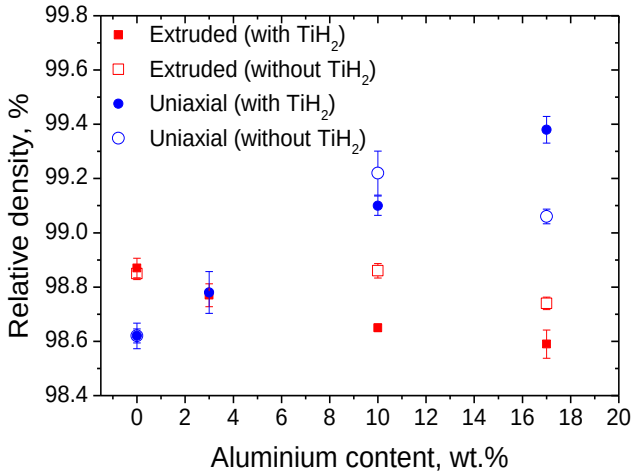

Figure 1. Relative density versus aluminium content of the alloys used, with distinction between manufacturing methods and blowing agent content.

3.2 Foam structure

A reasonable foam structure was achieved only by using extruded samples and applying PIF, see Table 1. Representative macrostructures of these foams are shown in Figures 4 and 5 and are compared to those produced from uniaxially pressed samples. The latter show only cracks and few large bubbles. Among all conditions tested, only one condition yielded in pure Mg foam with a reasonable foam structure, see Figure 4. Mg foam has a thick outer skin. The foams became coarser with increasing Al content as seen in Figures 4 and 5. In some conditions foam collapsed after maximum expansion and during solidification although they showed good expansion and a reasonable foam structure in the liquid state, see Table 1. One such example is shown in Figure 6.

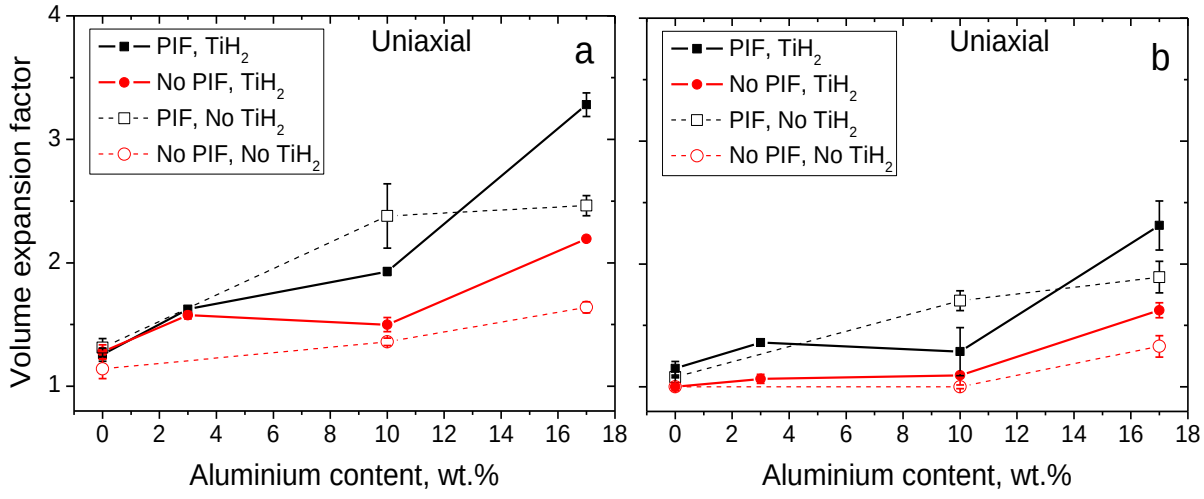

Figure 2. Expansion of uniaxially pressed precursors as a function of aluminium content, (a) maximum expansion, (b) end expansion.

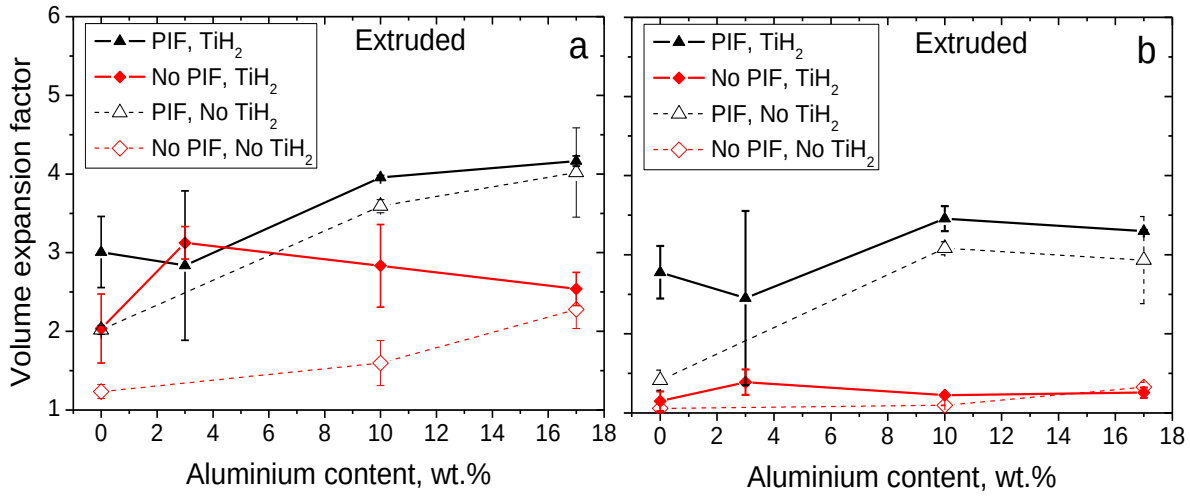

Figure 3. Same as Figure 2 for extruded precursors.

4 Discussion

4.1 Effect of compaction method

Magnesium is close packed hexagonal and therefore the number of the independent basal slip systems is less than required for uniform deformation [5]. In addition, sintering of Mg is strongly inhibited by a stable oxide layer [17]. Therefore consolidation of Mg powder is difficult. Compaction conditions have a significant effect on foaming behaviour [18,19]. One goal of compaction is to rupture the oxide layers on the surface of the metal powders, and to establish a metallurgical bonding among the metal powders by means of solid state diffusion which increases the strength of the precursor. If the strength of the precursor is not sufficient, crack-like pores appear due to the gas pressure generated during heating, and part of the gas is lost through these cracks leading to “bad” foams [20].

In uniaxial compaction material is deformed mainly by directed compressive stresses, whereas during extrusion of round rods biaxial stresses develop and oxide layers on powder surface are broken by the shearing action. This suggests that the quality of metallurgical bonding is better in extruded precursors than in uniaxially pressed ones. Consequently, during heating of uniaxially pressed samples cracks are created as can be seen in Figures 4 and 5. This does not occur for extruded samples. As a result, foaming of extruded samples is superior to that of uniaxially compressed samples as shown in Figures 2 and 3.

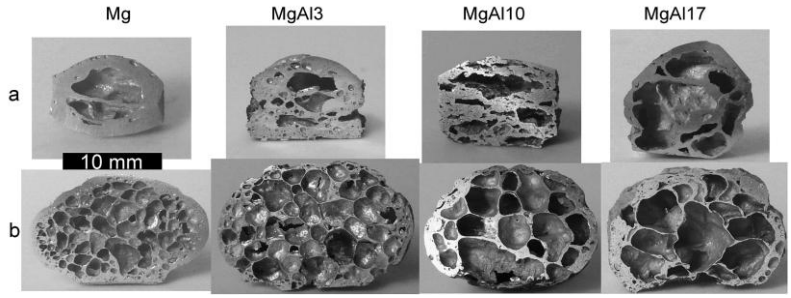

Figure 4. Comparison of macrostructures of foams produced by using PIF and precursors containing TiH_2, (a) uniaxially pressed and (b) extruded. (condition: PIF, TiH_2)

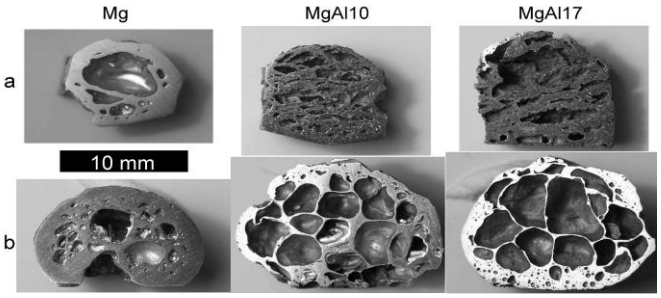

Figure 5. Comparison of macrostructures of the foams produced by using PIF and precursors without TiH_2, (a) uniaxially pressed and (b) extruded. (condition: PIF, No TiH_2)

4.2 Effect of Al content

Addition of Al to Mg increases the ductility of the alloy [5], which in turn improves consolidation. The soft Al improves consolidation by acting as plasticizer. Therefore the density of uniaxially pressed samples increased with Al content, see Figure 1. This trend was not observed for extrusion where compaction is not only by compressive but also by shear stress.

Beside precursors density, the appearance of the liquid phase during foaming plays an important role [21]. With the onset of melting samples get "sealed" by liquid phase which reduces gas losses [22]. Formation of liquid phase also ensures that as gas pressure is generated the compact expands or stretches rather than forming cracks. Since the solidus temperature decreases with increasing Al content (see Table 1), the gas is more efficiently used for foaming as the Al content increases. This is why foam expansion increases with increasing Al content as shown in Figures 2 and 3.

Coarsening of foam structure occurs through coalescence of smaller cells into a bigger cell. The longer time a foam spends in liquid state, the greater is the extent of coalescence, and as a result the coarser the foam becomes [23]. The alloys in this study have different melting ranges, see Table 1. The melting range of MgAl3 is 35 K, whereas for MgAl10 and MgAl17 it is about 120 K. Although all the alloys were foamed at a foaming temperature about 100 K above their liquidus point, MgAl10 and MgAl17 alloys spent more time in the semi-solid state. This resulted in a coarser macrostructure for these alloys as shown in Figures 4 and 5. The same trend is observed in Figure 6.

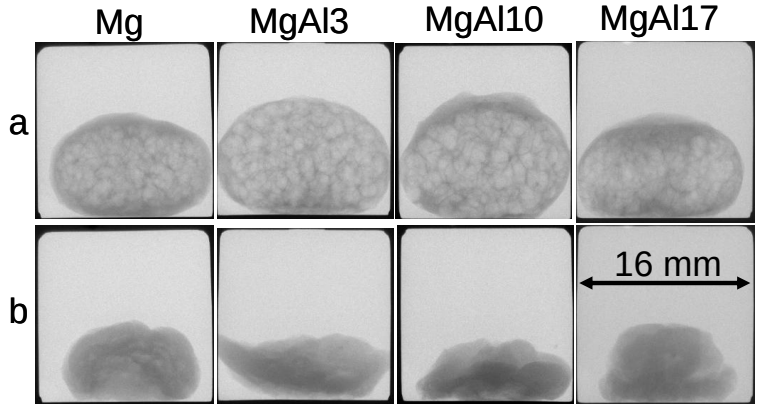

Figure 6. X-ray images of the foams produced from precursors containing TiH_2 and produced by extrusion. Foaming was performed under ambient pressure. (a) at maximum expansion state, (b) after solidification. (condition: No PIF, TiH_2)

4.3 Influence of foaming method

PIF allows foaming of blowing agent free precursors because of the release of gases adsorbed on metal powder surfaces [15]. In the presence of Mg additional gas sources are available in the form of MgH_2 [24]. Gas generated from these additional sources is preserved only when the precursor is melted under elevated pressure, e.g. 10 bar. In the case of ambient pressure foaming, most of this gas is lost. For this reason, for a given precursor, PIF method results in a higher foam expansion than ambient pressure foaming as observed in Figures 2a and 3a. Obviously, the blowing agent free precursors did not foam without applying PIF.

In the liquid state, a foam loses gas through out-diffusion of hydrogen. The rate of diffusion in Al alloy foams is controlled by an outer surface oxide layer, which slows down gas losses [13]. Note that although foaming was done in argon atmosphere, slight oxidation of Mg could not be avoided. In Mg or Mg-Al foams the outer oxide layer is MgO, which has a Pilling-Bedworth ratio of 0.8, i.e., < 1 [25], unlike Al_2O_3 where it is > 1. Therefore the MgO surface layer breaks and exposes molten Mg. This suggests that the gas losses in Mg-Al foams are controlled by the diffusion through molten Mg or Mg-Al which is fast due to a large diffusion coefficient of hydrogen in molten Mg (1.5×10^{-8} m^2s^{-1} at 650 ℃ [26]). A large amount of gas loss during foaming and solidification is another hindrance for foaming of Mg and Mg-Al alloys. It was possible to foam extruded precursors due to better consolidation, but the maximum achievable expansion was reduced by gas losses. In Figure 3a, for the "No PIF, TiH_2" condition, foams showed good expansion values. However due to loss of gas foams collapsed as evident from their final state expansion in Figure 3b and the X-ray images in **Figure 6**. For the "PIF, TiH_2" and "PIF, No TiH_2" conditions (Figure 3) gas losses were compensated by the generation of additional gas as discussed earlier. This made it possible to obtain Mg and Mg-Al alloy foams.

5 Summary

Mg and Mg-Al alloy foams with 60–70% porosity were produced. Among all the conditions tested, pure Mg foams with good expansion and satisfactory foam structure could only be produced from extruded samples containing TiH_2 and by pressure induced foaming. All the Mg-Al alloys prepared by extrusion yielded good foam structure only when PIF was applied, not by foaming at ambient pressure. Expansion increased with Al content. None of the uniaxially compacted samples resulted in stable foam regardless which foaming technique was applied.

6 References

[1] D.-H. Yang, Y. Shang-Run, W. Hui, M. Ai-Bin, J. Jing-Hua, C. Jian-Qing and W. Ding-Lie, *Mater. Sci. Eng. A* **527**, 5405 (2010).

[2] M. P. Staiger, A. M. Pietak, J. Huadmai and G. Dias, *Biomater*. **27**, 1728 (2006).

[3] C. E. Wen, M. Mabuchi, Y. Yamada, K. Shimojima, Y. Chino and T. Asahina, *Scripta Mater.* **45**, 1147 (2001).

[4] C. E. Wen, Y. Yamada, K. Shimojima, Y. Chino, H. Hosokawa and M. Mabuchi, *Mater Lett*. 2004;58:357.
[5] H. E. Friedrich and B. L. Mordike, Magnesium technology: metallurgy, design data, applications: Springer Verlag Berlin Heidelberg (2006).
[6] Z. G. Xu, J. W. Fu, T. J. Luo and Y. S. Yang, *Mater Design* **34**, 40 (2012).
[7] C. Körner, M. Hirschmann, V. Bräutigam and R.F. Singer, *Adv. Eng. Mater.* **6**, 385 (2004).
[8] K. Renger and H. Kaufmann, *Adv. Eng. Mater.* **7**, 117 (2005).
[9] Y. Yamada, K. Shimojima, Y. Sakaguchi, M. Mabuchi, M. Nakamura, T. Asahina, T. Mukai, H. Kanahashi and K. Higashi, *Mater. Sci. Eng. A*, **280**, 225 (2000).
[10] F. W. Bach, D. Bormann and P. Wilk, (eds. J. Banhart, N. A. Fleck) Cellular Metals and Metal Foaming Technology: MIT-Verlag, (2003). p.215.
[11] C. Jiménez, F. Garcia-Moreno, B. Pfretzschner, M. Klaus, M. Wollgarten M, I. Zizak, G. Schumacher, M. Tovar and Banhart, *Acta Materialia*, **59**, 6318 (2011).
[12] B. Matijasevic and J. Banhart, *Scripta Mater* **54**, 503 (2006).
[13] M. Mukherjee, F. Garcia-Moreno and J. Banhart, *Metal Mater Trans. B*, **41**, 500 (2010).
[14] T. R. Neu, Bachelor Thesis, Technische Universität Berlin (2010).
[15] F. Garcia-Moreno and J. Banhart, *Coll. Surf. A*, **309**, 264 (2007).
[16] F. García Moreno, M. Fromme and J. Banhart, *Adv. Eng. Mater.* **6**, 416 (2004).
[17] M. Wolff, T. Ebel and M. Dahms, *Adv. Eng. Mater.* **12**, 829 (2010).
[18] H. M. Helwig, S. Hiller, F. Garcia-Moreno and J. Banhart, Metal. *Mater. Trans. B* **40**, 755 (2009).
[19] C. Jiménez, F. Garcia-Moreno, M. Mukherjee, O. Goerke and J. Banhart, *Scripta Mater.* **61**, 552 (2009).
[20] L. Helfen, T. Baumbach, P. Pernot, P. Cloetens, H. Stanzick, K. Schladitz and J. Banhart, *J. App. Phy. Lett.* **86,** 231907 (2005).
[21] H. M. Helwig, F. Garcia-Moreno and J. Banhart, *J. Mater. Sci.* **46**, 5227 (2011).
[22] C. Jiménez, F. Garcia-Moreno, B. Pfretzschner, P. Kamm, T. R. Neu, M. Klaus, Ch. Genzel, A. Hilger, I. Manke and J. Banhart, Metfoam 2011. Busan, South Korea, 2011 (submitted).
[23] F. Garcia-Moreno, E. Solorzano and J. Banhart *J. Soft Matter.* (2011). doi: 10.1039/c1sm05831b
[24] M. Mukherjee, F. Garcia-Moreno, C. Jiménez and J. Banhart, *Adv. Eng. Mater.* **12**, 472 (2010).
[25] Y. Zhu, H. Lu, Q. Jiang, K. Mimura and M. Isshiki, *J. Electrochemical Soc.* **154**, C153 (2007).
[26] V. Ivanchenko and L. Rokhlin, Al-H-Mg, (eds. G. Effenberg, S. Ilyenko), Light Metal Ternary Systems: Phase Diagrams, Crystallographic and Thermodynamic Data, vol. 11A3 (2005).